ACADEMY OF SCIENCES OF THE USSR

P. N. LEBEDEV PHYSICAL INSTITUTE

I.E.Tamm Department of Theoretical Physics

High Energy and Cosmic Ray Physics

Preprint No 52

TOPONIUM SPECTROSCOPY AND QCD

A.A.Bykov, I.M.Dremin, A.V.Leonidov

Moscow, 1983

High Energy and Cosmic Ray Physics

Preprint No 52

TOPONIUM SPECTROSCOPY AND QCD

A.A.Bykov, I.M.Dremin, A.V.Leonidov

Moscow, 1983

TOPONIUM SPECTROSCOPY AND QCD

A.A.Bykov, I.M.Dremin, A.V.Leonidov

ABSTRACT

The energy levels of toponium *) and their leptonic widths are calculated in the framework of non-relativistic potential model. We compare results, obtained using various interpolations of renormgroup' β -function and various purely phenomenological potentials, in the wide interval of the awaited masses of toponium. All results are obtained within a uniform computational scheme. The sensitivity of results to specific features of QCD is discussed.

*) Toponium is a bound state $t\bar{t}$, formed by a hypothetic superheavy t -quark..

I. INTRODUCTION

The spectroscopy of mesons containing heavy quarks is often studied in the framework of nonrelativistic potential model, which provides good accuracy in the description of energy levels, relative leptonic widths and other characteristics (see, e.g., [1]). Special attention was paid to the spectroscopy of heavy vector resonances J/ψ and Υ. The form of the potential was dictated either by purely phenomenological reasons [2- 4, 19-21], or in accordance with QCD (small distances) and string models (large distances) [5 - 11].

The nonrelativistic potential model of quarkonia can provide with information about the behaviour of QCD coupling constant (see appendix B), effective renormalization structure, etc. Of a special interest is a possibility of checking our theoretical prejudices of the behaviour of the renormgroup β -function (see sect.II).

Previously, some interpolation formulas for $\beta(\rho)$ ($\rho = g^2/(4\pi)^2$ and g^2 is QCD coupling constant) with([6-9]), and without free parameters([10, 11]) were derived. In the literature one can also find $\beta(\rho)$, calculated in lattice QCD (see, e.g. [12]).

The general conclusion is that in the energy region of Υ one can't distinguish phenomenological potentials from those obtained from the interpolations of β-functions (with the only exception of a "lattice" potential), because they provide almost identical spectra.

In order to distinguish potentials and to choose the

correct one, one should descend to the domain of smaller distances (larger masses), see fig.2. From modern experimental data we know, that if toponium found, its mass must be larger than 37 GeV. It means that its spectroscopy will be much richer than those of J/ψ and Υ, i.e. it will tell us much more about the interquark potential.

The proof of the form of the potential at very small distances (for superheavy quarks) is important for QCD, as it is a simultaneous check of the flavour independence of the potential and (even more important) of the decrease of interaction at small distances (asymptotical freedom). As it is shown below, the properties of toponium enable us to distinguish potentials with asymptotically free behaviour from those without it. Let us mention, that an attempt of doing this [13] by the inverse scattering method starting from the well-established properties of Υ has failed. The properties of Υ permit any extrapolation (e.g. [2-11,19-21]) to smaller distances (< 0.1 fm).

The main goal of this paper is to study the properties of toponium in non-relativistic potential model using the same computational procedure for all the potentials considered. The interval of possible toponium masses from 40 to 60 Gev is investigated. Simultaneously the dependence of properties of Υ on the choise of interpolation of β -function is considered. In sect II we briefly discuss the correspondence between $\beta(g)$ and interaction potential and describe the spectrum of Υ and the leptonic widths of its S -levels, obtained using both parameterless interpolation formulas for β -functions, proposed in [10, 11], and lattice β -function [14]. Sect.III

contains results of computation of toponium energy spectra using various interpolation formulas for β -function [9-11]. and explicit analytic potentials[2-4,7,20,21]. In sect.IV the results for S -level leptonic widths of toponium are given. Sect. V contains the data on wave functions, bound energies, mean square radii of toponium and on the dependence of the effective coupling constant on the interquark separation.

Sect. VI is devoted to the discussion of the results obtained.

In app. A we compile the explicit analytical formulas for the potentials and for the interpolations of β -functions used.

In app. B we review the general formalism of the so-called "phase method" of numerical solution of Schrö-dinger equation.

In app. C we discuss the possibility of reconstruction of the static interaction potential from Feynman diagram with one-gluon exchange.

II. The estimate of the quark velocities in heavy quarkonia supports the possibility of applying the non-relativistic potential approach, that is to solve Schrö-dinger equation with adjustable potential. It provides an opportunity (see app. C) to establish the correspnndence between the experimental data and some prejudices on the structure of QCD. Particularly, it is possible to calculate the energy spectrum and other characteristics of heavy quarkonia with the chosen form of β -function. Let us recall, that the static potential is given by the formula:

$$V(r) = -32/3 \cdot \int_0^\infty \rho(Q^2)\ \frac{\sin(Q\cdot r)}{Q\cdot r}\, dQ \qquad (1)$$

where $\rho(Q^2) = g^2(Q^2)/(4\pi)^2$, g is QCD coupling constant depending on momentum transfer. The dependence of ρ on Q^2 is determined (with assumed $\beta(\rho)$) from the RG equation [15]

$$Q^2 \partial\rho/\partial Q^2 = \beta(\rho) \qquad (2)$$

In the weak coupling limit (small ρ) the β -function is calculated in perturbative QCD (see, e.g. [15]). In the strong coupling limit $\beta(\rho)$ is usually defined by the linearly rising part of interquark potential.

In the literature one can find various analytical interpolations of $\beta(\rho)$ between the two limits [6, 8, 10, 11, 14]. Both the explicit interpolation formulas and the list of all potentials used are reproduced in app. A. The various interpolations of β -functions are shown in fig.1; the most widely used potentials are shown in fig.2.

The interpolations of refs. [6, 8] contain free parameters, which are fixed in such way, that the spectrum of Υ is reproduced. The parameterless potentials [10, 11] have never been compared before with the data on Υ family. They differ from each other by the account in [11] of the Coulomb correction

---

x) Though there appears a sizeable imaginary part of the potential due to the string breaking and to the creation of quark-antiquark pairs.

to the string potential at large distances computed in [16]. We have carried out necessary computations and represent in table 1 the energy spectrum and leptonic widths of Υ -family. One can see, that interpolations suggested in [10, 11] provide a reasonably good fit. (An account of Coulomb correction to the potential improves agreement with experiment, so that in what follows we use the potential with this correction). Let us mention, that the coefficient a in the linearly rising term is the same as in the Cornell group analytical parameterization (see app.A), i.e. $a \simeq 0.14$ Gev^2, where the mass of b -quark is $m_4 = 4,43$ GeV. It is very essential that the slope a is in one-to-one correspondence with the value of the well-known QCD parameter Λ, which appears in the formula for the asymptoticaly free regime of the coupling constant $\alpha_s \sim \ln^{-1}(Q^2/\Lambda^2)$ when $Q^2 \to \infty$:

$$\Lambda^2 = C(n_f) \cdot a \qquad (3)$$

where n_f is a number of active flavours and the values of $C(n_f)$ are given in app. A (see table 1A). With $n_f = 5$ we get $\Lambda = 610$ MeV that essentially differs from the value $\Lambda \sim 100$ MeV which is widely used in the description of high-energy processes. It appears to be impossible to reproduce the spectrum of Υ with $\Lambda \sim 100$MeV.

From fig.1 one can easily see, that the lattice interpolation of $\beta(g)$ essentially differs from all other interpolatinns, which reproduce the spectra of quarkonia. It is natural to suppose, then, that lattice β -function would not be reproduce correctly the properties of quarkonia. It has been confirmed by our computation [x]. Its results are reproduced in table 1.

x) The computational scheme used is discussed in app. B.

Summarizing, we can say that experimental data on Υ -family reject only the lattice β -function and do not discriminate other potentials of app. A. One can see, however, that all the potentials are essentially different at smaller distances typical for toponium (fig.2).

Our main goal is, after determining the properties of toponium for various potentials, to help in choosing the correct one when the corresponding experimental data appear.

III. In the framework of non-relativistic Schrö-dinger equation with various potentials, describing the properties of J/ψ and Υ (see app.A) we have computed the mass separations, leptonic widths, wave functions, binding energies and mean square radii of the $t\bar{t}$ bound states in the interval of t-quark mass from 20 to 30 GeV. Already from the information on the masses of different states of toponium one can derive important conclusions. For the static system one can see whether the potential has asymptotically free behaviour because asymptotically free potentials reveal sizeably smaller mass differencies for toponium than non-free potentials (fig.3).

In fig.3 the $2S-1S$ toponium levels mass difference is shown as a function of the mass of the ground state. We have also computed the NL-1S levels mass differencies for $N=2,3,4,\ldots$ and $L = S, P, D$. The typical linear dependence (reminding of a Coulomb case) and the relative ordering of the curves remain intact for all N and L. Let us mention, however, that the numerical proximity of the potentials does not necessarily lead to the nearness of the mass differences because of the

important role of the derivative of the potential at the range of the bound states. In table 1 we present the numerical values of the ground state masses and of the mass differences for some potentials for the interval of t-quark masses from 20 to 30 GeV [*] .

IV. In this section we present the results of computation of leptonic widths of NS-states of $t\bar{t}$ (N = 1,2,3,4) where the t-quark mass is taken to be 20, 26 and 30 Gev. The leptonic widths are calculated from Van-Royen-Weisskopf formula [17] with radiative corrections [**] [18]

$$\Gamma_{ee} = \Gamma_{ee}^{(0)} \cdot \left(1 - 64/3 \cdot \rho(2m_t)\right) \qquad (4)$$

where

$$\Gamma_{ee}^{(0)} = 16\pi e_t^2 \alpha^2 / M_{N,s}^2(t\bar{t}) \cdot |\Psi_{N,s}(0)|^2 \qquad (5)$$

where e_t is an electric charge of t -quark, α-is fine structure constant, $\Psi_{N,s}(0)$ is a wave-function of NS-state at $r=0$, $M_{N,s}(t\bar{t})$ is a mass of a resonance.

[*] For intermediate values of the mass the values of the splittings could be found by the linear interpolation of the values in the table.

[**] The detailed discussion of the role of relativistic and radiative corrections can be found in [9].

In figs. 4 and 6 and table 3 we present, correspondingly, the values of $\Gamma(NS)/\Gamma(1S)$, which do not depend on the radiative corrections and the numerical value of $\Gamma(1S)$ for m_t = 20, 26, 30 GeV.

From the data obtained one can see that leptonic widths depend nonlinearly on the ground state mass (while we got a linear dependence for the mass splittings) and are, therefore, more sensitive to the form of the potential.

V. We publish only brief information about the basic experimentally measured properties of toponium because of the natural limitations on the size of the preprint. We have also data on wave functions, binding energies and mean square radia of toponium in the interval of t -quark mass from 20 to 30 GeV. Part of this information can be found in table 4. In fig.5 the effective coupling constant is shown as a function of the momentum transfer between the quarks.

VI. In summary, we can make the following conclusions:

1. The comparison of the experimental data on toponium, when available, to the results of our computation will enable to choose either potentials with asymptotic freedom or those without it. For this purpose an accuracy in mass measurements $\sim$ 500 MeV is sufficient.

2. In order to distinguish potentials, belonging to one of two big groups, mentioned above, one needs approximately an order of magnitude higher accuracy of experimental data.

3 The most sensitive to the form of the potential characteristics are relative leptonic widths. (Earlier this conclusion has been made, e.g., by the authors of

ref.[9]) *).

4. The relative mass splitting of NL-1S levels is governed by the first derivative of the potential at the radius of a bound state.

5. The Υ -family spectra are well described by the parameterless interpolation from Refs.[10, 11] and are not reproduced when the lattice β -function is used.

The authors are grateful to I.V.Andreev for many discussions.

---

*) This work contains a very thorough discussion of various properties of toponium in the framework of non-relativistic potential model for potentials [1 , 8].

APPENDIX A.

Here we list the phenomenological potentials and interpolation formulas for the renormgroup β-function, which are widely exploited to describe properties of J/ψ and Υ -families and are used in this paper. Let us mention that our list is not exclusive. When choosing the potentials we were governed by following considerations:

1. First of all, we have chosen the potentials with distinctly different behaviour (see, e.g., [2] and [4]).

2. Among group of potentials with common behaviour in a large interval of distances and common typical properties we have chosen only one (e.g. among quasilogarithmic [2] and logarithmic [19] potentials we have chosen [2]).

3. Among various interpolation formulas for β-function having similar analytic form, one has been chosen (e.g. [6] and [11]).

Table A1

Values of $C(n_f)$

n_f	$C(n_f)$
4	3.200
5	2.614
6	1.914

I. Interpolation formulas for β-functions exploited in this paper:

1. W.Buchmüller et al.[8]

$$1/\beta(\rho) = b_1 e^{-c\rho}/(b_0^2\rho) - 1/(b_0\rho^2(1-\exp(-1/b_0\rho)))$$

where (see, e.g., Ref.[15]) $b_0 = (33-2n_f)/3$, $b_1 = (306-38n_f)/3$

n_f - number of flavours, $c = 24$.

2. I.M.Dremin et al. [11]

$$-\beta(\rho) = \left[\left(\frac{b_1+b_0^2}{1-\rho_0 b_0}\right)\rho^3 + b_0\rho^2\right] \Big/ \left[\left(\frac{b_1+b_0^2}{1-\rho_0 b_0}\right)\rho^2 + \left(\frac{b_0+\rho_0 b_1}{1-\rho_0 b_0}\right)\rho + 1\right]$$

where $\rho_0 = 1/64$ and is determined by the Coulomb correction to the string potential (see Ref.[16])

3. Lattice β -function has been reconstructed from the curve presented in Ref.[14].

II. Quark-antiquark interaction potentials exploited in this paper: *)

4. A.Martin [2]

$$V(r) = -8.064 + 6.8698\, r^{0.1}$$

5. E.Eichten et al. [4]

$$V(r) = -0.52/r + r/(2.34)^2$$

6. K.Krasemann et al. [20]

$$V(r) = \begin{cases} -\pi/25 \cdot 1/(r \ln r/r) + C_1 & r < 0.365 \\ 0.69 \ln r/r & 0.365 \le r \le 3.45 \\ 0.156\, r & r > 3.45 \end{cases}$$

*) All parameters and coefficients as well as the inverse qiark-antiquark separation are measured in GeV.

where $r_0 = 1.63$; $c_1 = 0.4$, $\mu = 2.54$

7. Cornell Group [21]

$$V(r) = -0.8/r + r/(2.88)^2$$

8. R.Levine et al. [7]

$$V(r) = 0.1768\,r - 1.093/\left[r \ln\left(\frac{2.384\,e^{-0.4022\,r}}{r} + 2.7182\right)\right]$$

9. A.Bhanot et al. [3]

$$V(r) = \begin{cases} -0.8/r & r < 0.9 \\ 0.846 \ln r/r_0 & 0.9 \leq r \leq 7.0 \\ r/(2.81)^2 & r > 7.0 \end{cases}$$

where $r_0 = 2.58$

APPENDIX B The computational method.

The numerical computation of eigenvalues and eigenfunctions of Shrödinger equation is a very complicated problem. The choice of the method radically influences the possibility of obtaining the result and its accuracy. The radial Shrödinger equation with boundary conditions is written as:

$$\begin{cases} \chi'' + \left(E - U_\ell(r)\right)\chi = 0 \\ \chi(0) = 0 \\ \chi(r)\big|_{r\to\infty} \to F(U_\ell) \end{cases} \qquad \text{(B1)}$$

where $\chi(r) = r \cdot R(r)$, $R(r)$ is a radial wave function, $U_\ell(r)$ is an interaction potential with the radial term, $F(U_\ell)$ defines the form of the boundary condition at infinity, it depends on the potential chosen. Let us use the following Ansatz:

$$\begin{cases} \chi(r) = g(r) \sin\varphi(r) \\ \chi'(r) = g(r) \cos\varphi(r) \end{cases} \qquad \text{(B2)}$$

where $g(r)$ and $\varphi(r)$ are to be found. The consistency of (B2) with (B1) leads to a system of two equations of the first order:

$$\begin{cases} \varphi' = \cos^2\varphi + (E - U_\ell)\sin^2\varphi \\ g' = -g \cdot (E - U_\ell - 1)\sin\varphi\cos\varphi \end{cases} \qquad \text{(B3)}$$

The first equation does not contain $g(r)$. In what follows we study only this equation. With the boundary conditions for $\chi(r)$ we have:

$$\begin{cases} \varphi' = \cos^2\varphi + (E - U_\ell)\sin^2\varphi \\ \varphi(0) = 0 \\ \varphi(r)\big|_{r\to\infty} = \operatorname{arctg}\left[\frac{\chi}{\chi'}\Big|_{r\to\infty}\right] \end{cases} \qquad \text{(B4)}$$

Instead of solving the eigen-value problem (B4) it is convinient to deal with two Cauchy problems with boundary conditions correspondingly at $r = 0$ (B5) and at $r \to \infty$ (B6).

$$\begin{cases} \varphi_0' = \cos^2\varphi_0 + (E - U_\ell)\sin^2\varphi_0 \\ \varphi_0(0) = 0 \end{cases} \qquad \text{(B5)}$$

$$\varphi_\infty' = \cos^2\varphi_\infty + (E - V_e)\sin^2\varphi_\infty$$

$$\varphi_\infty(r)\Big|_{r\to\infty} \to -\operatorname{arctg}\left[\frac{\chi}{\chi'}\Big|_{r\to\infty}\right] \qquad \text{(B6)}$$

It is necessary to add to (B5) and (B6) the continuity condition for logarithmic derivative of $\chi(r)$ at any $\tilde{r}$ in the interval $[0, \infty)$, which reads

$$\varphi_0(\tilde{r}, E) + \varphi_\infty(\tilde{r}, E) = \pi(n+1) \qquad \text{(B7)}$$

where $\tilde{r}$ is any point in $[0, \infty)$ and n is the number of zeroes of the wave function.

Equation (B7) is an algebraic equation for E . It is easily solved by the Newton method:

$$E^{(k+1)} = E^{(k)} - \left[\varphi_0(\tilde{r}, E^{(k)}) + \varphi_\infty(\tilde{r}, E^{(k)})\right] \Big/ \left[\frac{\partial}{\partial E^{(k)}}\left(\varphi_0(\tilde{r}, E^{(k)}) + \varphi_\infty(\tilde{r}, E^{(k)})\right)\right] \qquad \text{(B8)}$$

where $E^{(k)}$ and $E^{(k+1)}$ are the former and the latter interactions, correspondingly. The equation and the boundary conditions are obtained by differentiating (B5) and (B6) with respect to E . The main virtues of this method are:

a) The rapid convergence of the iteration procedure. The method is almost insensible to the input value of $E^{(0)}$ (it can even differ from the final value by an order of magnitude).

b) The method enables to find the only solution for fixed quantum numbers.

APPENDIX C

Here we discuss the correspondence between the potential model and QCD. The main suggestion is that we are able to extract the non-relativistic interaction potential of heavy quark and antiquark from the diagram with one-gluon exchange (fig.1C)

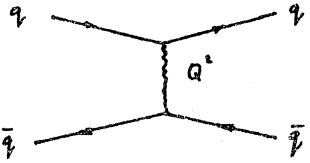

Fig.1C

In the non-relativistic limit we are, in fact, calculating the effective non-relativistic interaction potential [*] and use it in the Shrödinger equation [23]

$$V(K) \sim j_\mu \frac{1}{K^2} D_{\mu\nu} j_\nu \qquad (C1)$$

where $j_\mu \sim \bar{\psi}\gamma_\mu\psi$ is a fermionic current and $\frac{1}{K^2} D_{\mu\nu}$ - is a diagonal component of the gluon propagator. Let us treat the diagram 1C in the case when $D_{00} \neq 0$. Only this case will be considered in this paper. Then we immediately obtain:

$$V(\vec{K}) \sim g_0^2 D_{00}(\vec{K}) \qquad (C2)$$

Here g_0^2 is a bare coupling constant fixed at some normalization point. The three-momentum appears because the time-like component

---

[*] Its correspondence to the interaction energy of two infinitely massive quarks is not clear now due to possibility of relatively large non-perturbative effects [24].

K_0 of the interquark momentum exchange $K=(K_0,\vec{K})$ is proportional to $1/M$ where M is a mass of the quark, and in the leading approximation it can be omitted. At small distances $(K^2\to\infty)$ naturally appears Coulomb-like potential with asymptotically free effective coupling constant. Let us briefly discuss the role of radiative corrections in the limit $K^2\to 0$ (large distances). Extracting all renormalization factors of the diagram 1C and taking into account (C2) we get

$$V(K^2)\sim(Z_g)^2\cdot g_0^2\ \frac{1}{K^2}\ D_{00} \qquad (C3)$$

where $Z_g=\sqrt{Z_3}\cdot\left(Z_1^F/Z_1^{FVV}\right)$ is a charge renormalization factor, Z_3 - that of gluon propagator, $\left(Z_1^{FVV}\right)^{-1}$ - that of fermion-vector vertex (see, e.g., [23]).

Using the axial gauge (where $Z_2^F=Z_1^{FVV}$ due to Ward identity) we get:

$$V(K^2)\sim Z_3(K^2)\ \frac{g_0^2}{K^2}\left[g_{00}-\frac{2n_0K_0}{(nK)}+\frac{n_0^2K_0^2}{(nK)^2}\right] \qquad (C4)$$

where gauge-fixing vector n is taken to be spacelike: $n^2<0$. In the limit $K^2\to 0$ it was shown (see, e.g., [25]) that the behaviour $Z_3(K^2)\big|_{K^2\to 0}\sim\frac{1}{K^2}$ does not contradict (within some assumptions) the exact Schwinger-Dyson equations for gluon propagator.

In the static limit we have, therefore:

$$V(K^2)\big|_{K^2\to 0}\sim Z_3(K^2)\big|_{K^2\to 0}\cdot\frac{1}{K^2}\sim\frac{1}{K^4}$$

which means that $V(r)\sim r$ for large r. Therefore in the axial gauge the linear potential naturally arises from the diagram 1C if the radiative corrections in the limit $K^2\to 0$ are taken into account.

References

1. Martin A. TH. 3162-CERN, 16 September 1981
   TH. 3397-CERN, 26 August 1982.
2. Martin A. Phys. Letters. B100, p.511, 1981
3. Bhanot A., Rudaz K. Phys. Lett. B78, p.119, 1978
4. Eichten E., Gottfried K.., Kinoshita T., Zone K.D., Jan T.M. Phys. Rev. D21, p.203, 1980
5. Richardson J.L. Phys. Lett. B82, 1979, p.272.
6. Celmaster W., Henyey F. Phys. Rev. D18, p.1688, 1978
7. Levine R., Tomozawa J. Phys. Rev. D19, p.1572, 1979
   Phys. Rev. D21, p.840, 1980
8. Buchmüller W., Grunberg G., Tye S-H.H. Phys. Rev. Lett. 45 p.103, 45 p 587 (E) 1980
9. Buchmüller W., Tye S-H.H. Phys. Rev. D24 1981 p.132
10. Dremin I.M., Lebedev Inst. Reports N 1, 1982
11. Dremin I.M., Leonidov A.V. Theoretical and Mathematical Physics, 51, 178, 1982.
12. See, Bander M. Phys. Rep. 75 p.205 1981
13. Miller K.J., Olsson M.G. Phys. Rev. 25 p. 2382, 1982
14. Kovacz E., Phys. Rev. 1982, D25, p 871
15. See Reya E. Phys. Rep. 69, p.N 3, p.195, 1981
16. Lüsher M., Symanzik K., Weisz. P.. Nucl. Phys. B173 p.365 1980
    Lüsher M., Nucl. Phys. B180 p.317, 1981.
17. Van Royen V., Weiskopf W. Nuoco Cimento 50, p.617, 1967

18. Karplus R., Klein A. Phys. Rev. 87, p.848 1952
Barbieri R., Gatto R., Kögeler R., Kunzstz M., Phys. Letters B.57 p.455 1975
19. Quigg C., Rosner J.L., Phys. Rep. 56, 169, 1979.
20. Krasemann K., Ono K. Nucl. Phys. B154 p.283 1978
21. See, E.Eichten et al. Phys. Rev. D17 p 3090 1978
22. Kalitkin N.E. Methody vychyslenii. MGU, M., 1966.
23. Bander. M. Phys. Rep. 75. N 4. p.205 I98I.
24. Voloshin M.B. Nucl. Phys. B154,p.365, 1979.
25. Baker M., Zachariasen F., Phys. Rev. D17, 1978
26. Quigg C. et al. Phys. Rev. D18,274, 1978; D21,234, 1980; D 23,2625, 1981.

Figure and Table Captions

Fig. 1. The Interpolations of renormgroup β-function
1. W.Buchmüller et.al. [8]
2. I.M.Dremin et.al. [11]
3. "Lattice" β-function [14]

Fig. 2. The Interaction potentials of heavy quarks.
1. W.Buchmüller et.al. [8]
2. I.M.Dremin et.al. [11]
3. "Lattice" potential [14]
4. A.Martin [1,2]
5. E.Eichten et.al. [4]
6. K.Krasemann et.al. [20]
7. Cornell Group [21]
8. R.Levine et.al. [7]
9. A.Bhanot et.al. [3]

Fig. 3. The 2S-1S toponium mass splitting for various potentials(numbering of curves as in fig.2)

Fig. 4. The leptonic widths ratio of 2S-1S toponium levels for various potentials (numbering of curves as in fig.2)

Fig. 5. The effective coupling constant ρ as a function of the momentum transfer between quarks $-Q^2$

Table 1. The energy levels and leptonic widths of Υ family for parameterless [10, 11] and "lattice" potentials in comparison with experimental data.

Table 2. The ground state mass and the values of toponium mass splittings

Table 3. The leptonic widths ratios for nS and 1S states and the absolute value of leptonic width of 1S toponium state

Table 4. The binding energy and mean square radii of toponium.

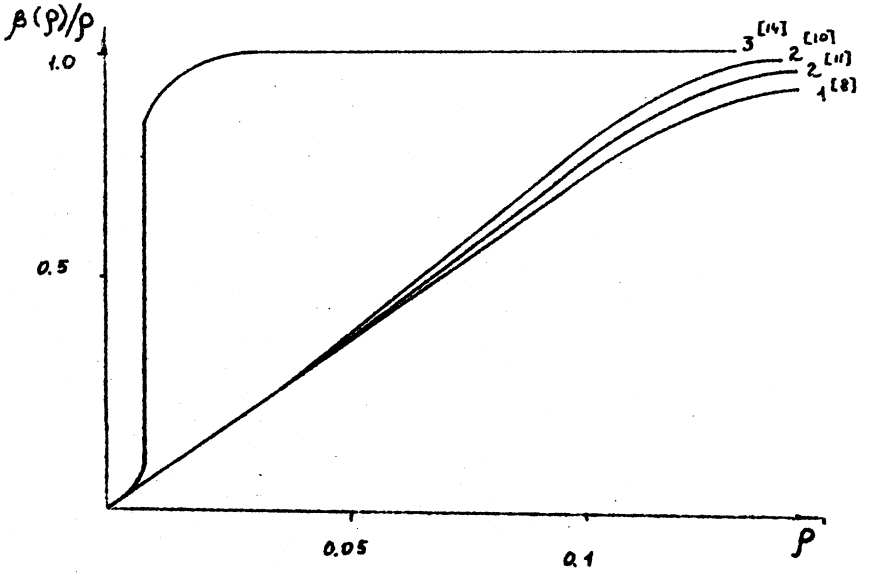
β(ρ)/ρ
1.0
0.5
3 [14]
2 [10]
2 [11]
1 [8]
0.05
0.1
ρ

Fig.I

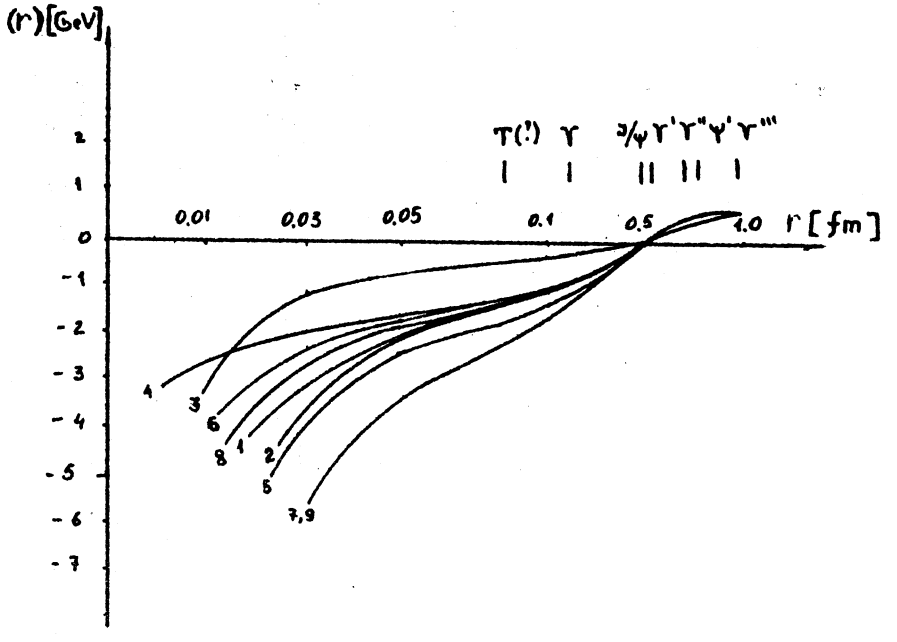
(r)[GeV]
2
1
0
-1
-2
-3
-4
-5
-6
-7
T(') ϒ ³/ψ ϒ' ϒ'' ψ' ϒ'''
0.01
0.03
0.05
0.1
0.5
1.0
r [fm]
4
3
6
8
1
2
5
7,9

Fig.2

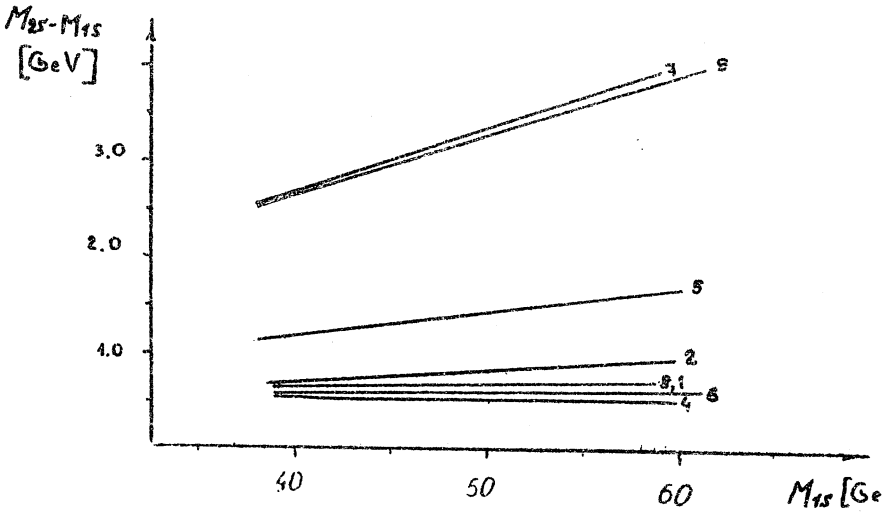
$M_{2S}-M_{1S}$ [GeV]
3.0
2.0
4.0
40
50
60
M_{1S} [Ge
7
8
5
2
8,1
4
6

Fig.3

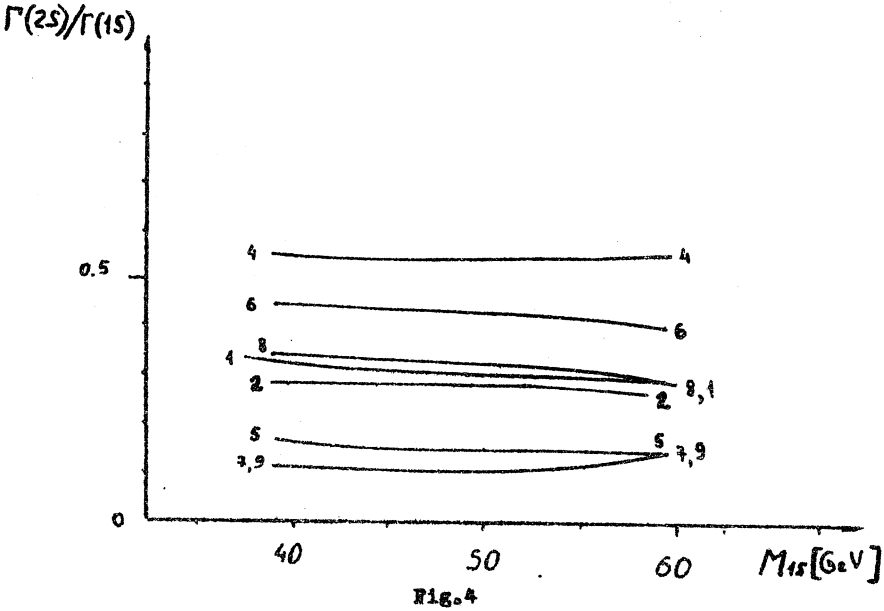
$\Gamma(2S)/\Gamma(1S)$
0.5
0
40
50
60
M_{1S}[GeV]
4
6
8
2
5
7,9
8,1

Fig.4

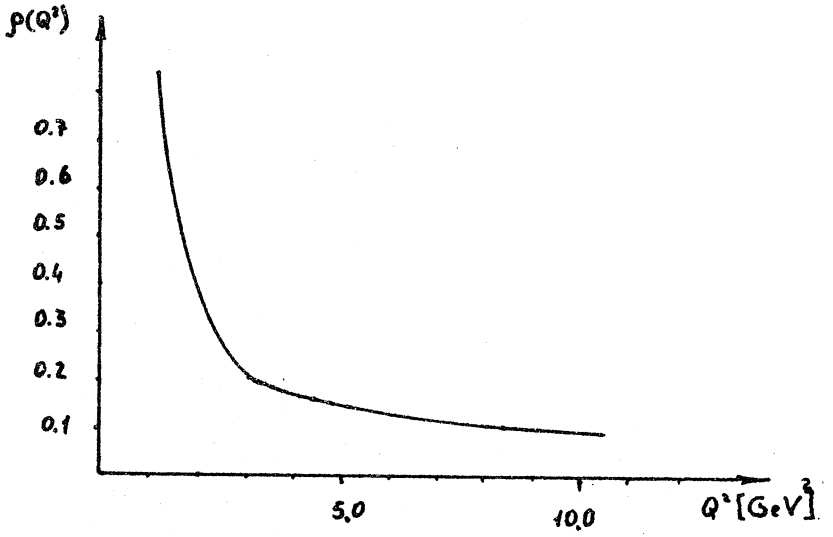

Fig.5

Table I.

State	Experiment	$_2$[II]	$_3$[I4]
M_{1S}, GeV	9.46	9.46 (9.46)	9.46
M_{2S}, -"-	I0.02	I0.02 (I0.02)	I0.02
M_{3S}, -"-	I0.35	I0.35 (I0.36)	I0.47
M_{4S}, -"-	I0.58	I0.6I (I0.62)	I0.86
M_{2P}, -"-	I0.25	I0.26 (I0.26)	I0.28
$\Gamma(1S)$, KeV	I.33±I.05	I.I3 (I.22)	0.3I
$\Gamma(2S)/\Gamma(1S)$	0.45±0.05	0.42 (0.42)	0.88
$\Gamma(3S)/\Gamma(1S)$	0.32±0.05	0.30 (0.3I)	0.79
$\Gamma(4S)/\Gamma(1S)$	0.24±0.05	0.24 (0.25)	0.72

x) The results for [I0] are written in brackets.

Table 2

States' masses [GeV]	m_t = 20 GeV					
	2^{11}	4^{2}	8^{7}	6^{20}	1^{8}	7^{21}
M_{1S}	40.243	38.652	39.099	39.427	39.068	36.822
$M_{2S} - M_{1S}$	0.723	0.540	0.643	0.582	0.674	2.467
$M_{3S} - M_{1S}$	1.020	0.851	0.965	0.895	0.989	3.010
$M_{4S} - M_{1S}$	1.207	1.075	1.200	1.111	1.209	3.278
$M_{1P} - M_{1S}$	0.641	0.387	0.546	0.462	0.576	2.452
$M_{2P} - M_{1S}$	0.967	0.746	0.890	0.813	0.920	2.995
$M_{3P} - M_{1S}$	1.168	0.994	1.135	1.048	-	3.263
$M_{4P} - M_{1S}$	1.316	1.185	1.334	1.228	-	3.449
$M_{1D} - M_{1S}$	0.908	0.677	0.746	0.676	0.843	2.967
$M_{2D} - M_{1S}$	1.121	0.913	1.064	0.977	1.089	3.237
$M_{3D} - M_{1S}$	1.275	1.119	1.270	1.169	-	3.423
$M_{4D} - M_{1S}$	1.409	1.286	1.447	1.325	-	3.575

	m_t = 30 GeV					
M_{1S}	59.522	58.522	58.861	59.242	58.818	55.214
$M_{2S} - M_{1S}$	0.950	0.528	0.722	0.611	0.762	3.646
$M_{3S} - M_{1S}$	1.318	0.836	1.048	0.930	1.090	4.383
$M_{4S} - M_{1S}$	1.540	1.059	1.277	1.151	1.309	4.702
$M_{1P} - M_{1S}$	0.847	0.381	0.632	0.505	0.668	3.636
$M_{2P} - M_{1S}$	1.252	0.733	0.982	0.857	1.026	4.373
$M_{3P} - M_{1S}$	1.495	0.978	1.221	1.092	-	4.692
$M_{4P} - M_{1S}$	1.678	1.176	1.420	1.283	-	4.898
$M_{1D} - M_{1S}$	1.184	0.633	0.906	0.765	0.955	4.353
$M_{2D} - M_{1S}$	1.442	0.898	1.157	1.022	1.200	4.673
$M_{3D} - M_{1S}$	1.629	1.103	1.357	1.217	-	4.877
$M_{4D} - M_{1S}$	1.813	1.300	1.553	1.409	-	5.059

Table 3

Ratio	m_t = 20 GeV					
	$_2$[11]	$_4$[2]	$_8$[7]	$_6$[20]	$_1$[8]	$_7$[21]
$\Gamma(1S)$, keV	7.105	1.479	4.863	3.350	5.100	108.65
$\Gamma(2S)/\Gamma(1S)$	0.283	0.552	0.355	0.450	0.330	0.120
$\Gamma(3S)/\Gamma(1S)$	0.157	0.390	0.234	0.290	0.210	0.046
$\Gamma(4S)/\Gamma(1S)$	0.111	0.304	0.186	0.219	0.160	0.029

Ratio	m_t = 26 GeV					
	$_2$[11]	$_4$[2]	$_8$[7]	$_6$[20]	$_1$[8]	$_7$[21]
$\Gamma(1S)$, keV	8.083	1.251	5.228	3.486	5.341	141.85
$\Gamma(2S)/\Gamma(1S)$	0.277	0.548	0.324	0.432	0.310	0.115
$\Gamma(3S)/\Gamma(1S)$	0.151	0.396	0.206	0.275	0.190	0.041
$\Gamma(4S)/\Gamma(1S)$	0.108	0.314	0.161	0.205	0.140	0.024

Ratio	m_t = 30 GeV					
	$_2$[11]	$_4$[2]	$_8$[7]	$_6$[20]	$_1$[8]	$_7$[21]
$\Gamma(1S)$, keV	9.374	1.125	5.470	3.665	5.680	151.60
$\Gamma(2S)/\Gamma(1S)$	0.276	0.558	0.308	0.409	0.300	0.116
$\Gamma(3S)/\Gamma(1S)$	0.151	0.399	0.193	0.258	0.180	0.039
$\Gamma(4S)/\Gamma(1S)$	0.102	0.330	0.150	0.198	0.130	0.022

Table 4

State	$\langle r^2 \rangle^{1/2}$ fm , m_t = 26 GeV					
	$_2$[11]	$_4$[2]	$_8$[7]	$_6$[20]	$_1$[8]	$_7$[21]
1 S	0.073	0.107	0.081	0.093	0.078	0.033
2 S	0.200	0.229	0.209	0.215	0.205	0.122
3 S	0.340	0.346	0.333	0.340	0.343	0.246
4 S	0.474	0.461	0.447	0.463	0.467	0.384
1P	0.161	0.175	0.166	0.170	0.165	0.101
2 P	0.298	0.292	0.292	0.295	0.295	0.228
3 P	0.437	0.410	0.408	0.420	0.441	0.366
4 P	0.537	0.512	0.504	0.519	0.50	0.491
1 D	0.240	0.236	0.241	0.237	0.242	0.190
2 D	0.382	-	0.362	0.367	0.371	0.334
3 D	0.505	0.473	0.471	0.484	0.493	0.466
4 D	0.541	0.540	0.535	0.540	0.537	0.539
	E_b GeV, m_t = 26 GeV					
1 S	0.064	-1.432	-1.050	-0.691	-1.064	-4.139
2 S	0.888	-0.901	-0.360	-0.092	-0.346	-0.972
3 S	1.207	-0.591	-0.036	0.225	-0.024	-0.314
4 S	1.404	-0.369	0.193	0.443	0.194	-0.016
1 P	0.798	-1.049	0.452	-0.203	-0.441	-0.982
2 P	1.152	-0.694	-0.105	0.149	-0.091	-0.325
3 P	1.362	-0.449	0.135	0.383	0.124	-0.028
4 P	1.521	-0.257	0.330	0.567	0.325	0.168
1 D	1.092	-0.797	-0.184	0.056	-0.164	-0.347
2 D	1.318	-	0.069	0.313	0.080	-0.049
3 D	1.480	-0.326	0.269	0.505	0.256	0.146
4 D	1.641	-0.147	0.451	0.680	0.445	0.312

Т - 21645

Подписано в печать 18 декабря 1982 года

Заказ № 108. Тираж 100 экз. п/л 1,3

Отпечатано в Редакционно-издательском отделе ФИАН СССР

Москва, В-312, Ленинский проспект, 53